CLEAN TECHNOLOGY, Vol. 14, No. 3, September 2008, pp. 153~159

초임계이산화탄소내 트리클로산의 용해도와 미세입자 제조공정의 응용

신문삼, 김화용*

서울대학교 화학생물공학부
151-744 서울시 관악구 신림동 산56-1

(2008년 8월 25일 접수; 수정본 접수일 9월 12일; 2008년 9월 18일 채택)

Solubility of Triclosan in Supercritical Carbon Dioxide and its Application to Micronization Process

Moon Sam Shin and Hwayong Kim*

School of Chemical and Biological Engineering, Seoul National University
San 56-1, Shinlim-dong, Gwanak-gu, Seoul 151-744, Korea

(Received for review August 25, 2008; Revision received September 12, 2008; Accepted September 18, 2008)

요 약

여드름 치료제인 트리클로산의 초임계이산화탄소에 대한 용해도를 가변부피셀(Variable volume cell)을 이용하여 온도 313.15, 323.15와 333.15 K에 대해서 10 - 40 MPa 압력범위에서 측정되었다. QLF (Quasi-chemical nonrandom lattice fluid) 상태방정식을 이용하여 측정된 용해도를 잘 계산할 수 있었고, 이 자료를 미세입자공정에 활용하였고, 입자크기에 미치는 온도와 압력의 효과를 해석하였다.

주제어 : 트리클로산, 초임계유체, 이산화탄소, 용해도, 미세입자

Abstract : The solubility of triclosan, an anti-acne agent was measured in supercritical carbon dioxide ($scCO_2$) with a variable volume view cell at 313.15, 323.15, and 333.15 K and at pressures between 10 and 40 MPa. We successfully correlated triclosan solubility in $scCO_2$ using the quasi-chemical nonrandom lattice fluid (QLF) equation of state. Triclosan was micronized using the rapid expansion of supercritical solutions (RESS) process. The effects of temperature and pressure on particle size were investigated using phase behavior data and correlated results from the QLF model.

Key words : Triclosan, Supercritical fluids, Carbon dioxide, Solubility, Micronized particles

1. INTRODUCTION

Micronized particles are used in various fields, such as cosmetics, pharmaceuticals, food supplements and electronics[1]. Various processes for fine particles using supercritical fluids (SCF) have been studied[2-5], including supercritical anti-solvent (SAS) and rapid expansion of supercritical solutions (RESS). Micronized processes of the biomaterials can enhance the dissolution rates of biomolecules into the biological environment. Dissolution rate is a function of the surface area of particles and solubility. The surface area can increase through the reduction of particle size. It has been reported the RESS process can be used to micronize biomaterials such progesterone and cholesterol[6].

Triclosan is a diphenyl ether (bis-phenyl) derivative, known as either 2,4,4'-Trichloro-2'-hydroxy diphenyl ether or 5-Chloro-2-(2,4-dichlorophenoxy) phenol and has been widely used as anti-acne agent[7, 8] in pharmaceutical and cosmetic products. Triclosan is white crystalline powder and has poor solubility in water. The dissolution rate of triclosan can be improved by the reduction of particle size.

* To whom correspondence should be addressed.
E-mail: hwayongk@snu.ac.kr

Solubility information is essential for choosing a supercritical fluid processes for particle design. The solid solubility in supercritical fluid can be calculated by the equation-of-state (EOS) method such as Peng and Robinson EOS[9]. Most recently, the present authors presented a quasi-chemical nonrandom lattice fluid (QLF) EOS[10,11] and found that the QLF EOS successfully modeled the solubility of biological compounds in supercritical fluid [12].

In this study, the equilibrium solubility of triclosan was measured in supercritical carbon dioxide with static method in the pressure range from (10 to 40) MPa and at temperatures of (313.15, 323.15, and 333.15) K. Triclosan was micronized using the rapid expansion of supercritical solutions (RESS) process. The effects of temperature and pressure on particle size were investigated using phase behavior data and correlated results from the QLF model.

2. EXPERIMENTAL SECTION

2.1. MATERIALS

Carbon dioxide (min. 99.5%) was supplied from Korea Industrial Gases. Triclosan (min. 97.0%) was supplied by Ciba Specialty Chemical. These materials were used without further purification.

2.2. SOLUBILITY MEASUREMENT

The cloud point of triclosan in $scCO_2$ was measured using a high pressure apparatus installed a variable volume view cell[12]. As shown in Figure 1, the cell is equipped with two sapphire windows to enable observation of the turbidity of the solution as pressure is reduced, a movable piston to change pressure, a magnetic stirring bar and a pressure generator (High Pressure Equipment Co., 50-6-15). In addition, a cooling jacket was installed to minimize heat transfer and maintain a constant temperature in the cell. The system temperature was measured by a K-type thermocouple (accuracy of ±0.045 K) and The system pressure was measured using a high pressure precision gauge (Honeywell Sensotec Co., TJE). In our previous studies, this apparatus was used in phase behavior of polymer + monomer + carbon dioxide [13], and fluoroalcohol + carbon dioxide systems [14]. The experiment was performed as follows: after the addition of a fixed amount (within the precision of ±0.00001 g) of triclosan into the cell, the cell was purged with CO_2 gas to remove trapped air and known volumes of CO_2 (within the precision of ±0.00001 g using a high-pressure bomb) were then charged into the cell. The solution in the cell was agitated by the magnetic bar and heated to the desired temperature. After the solute was dissolved and the solution was maintained as a single phase, the pressure was slowly reduced by moving the piston located within the cell using the pressure generator until the solution became cloudy. The solubility of triclosan in $scCO_2$ was determined by observing the cloud point which is defined as the pressure at which it is no longer possible to observe the magnetic bar [12]. When the cloud point was observed, the solubility was calculated using the known amount of solid loaded into the vessel along with the amount of carbon dioxide present in the vessel. After each cloud point observation, the view cell was vent, thoroughly cleaned, and dried. This procedure was repeated several times until the fluctuation of phase transition pressure was minimized to within ±0.05 MPa.

2.3. RESS EXPERIMENT

A schematic diagram of the experimental apparatus used for the RESS process is shown in Figure 2. The apparatus mainly consists of a CO_2 supplying system, a pressure system, a dissolution vessel, an expansion system and an expansion chamber

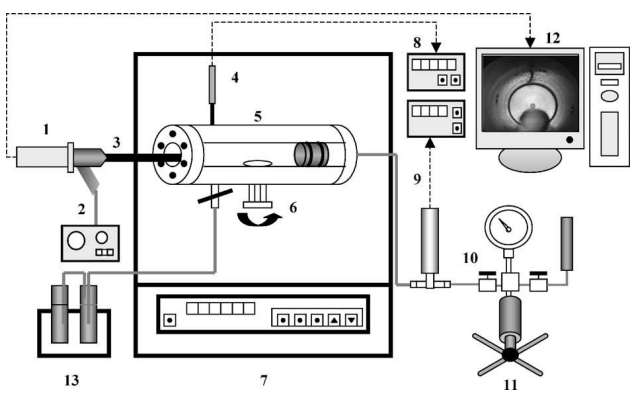

Figure 1. Schematic diagram of experimental apparatus.
(1) camera; (2) light source; (3) borescope; (4) fast response PRT; (5) viewcell; (6) magnetic stirrer; (7) air bath; (8) digital thermometer; (9) digital pressure transducer; (10) pressure gauge; (11) hand pump;(12) computer monitor; (13) trap.

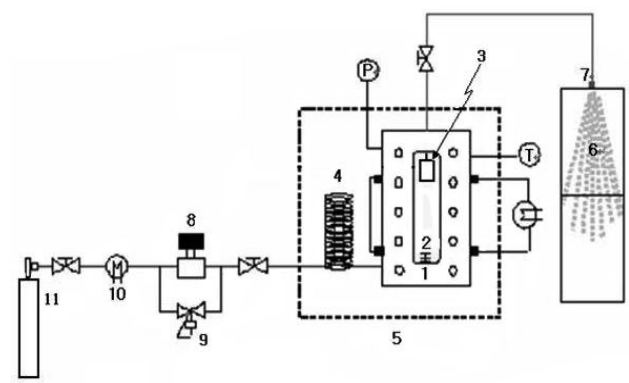

Figure 2. Schematic diagram of RESS apparatus.
(1) dissolution vessel; (2) magnetic bar; (3) filter (0.5μm); (4) pre-heater; (5) air bath; (6) expansion chamber; (7) nozzle; (8) pump; (9) back pressure regulator; (10) circulating bath; (11) CO_2 cylinder.

in which the particle are collected. CO_2 is supplied from a gas cylinder and the gaseous CO_2 liquefied through a cooler (Jeio Tech. Co. Ltd, RW-0525G) set to -10℃. CO_2 was pressured by a diaphragm metering pump (Pulsafeeder Inc, PULSA 680). A back pressure regulator (Tescom Corp., 26-1761-24-161) was installed after the pump exit. After the pressured CO_2 passed through the back pressure regulator, it was delivered to the dissolution vessel. Prior to entering the dissolution vessel, the CO_2 passed through a pre-heater to minimize temperature difference of the injected CO_2 and the interior of the dissolution vessel. The temperature of solution in dissolution vessel was controlled by thermostatic circulating water in the jacket using a refrigerated circulating bath. System temperature was measured by a K-type thermocouple. The magnetic bar was used to accelerate the dissolution rate of triclosan. A metal fritted filter was installed between the dissolution vessel and the valve so that only triclosan dissolved was passed through the filter. Once $scCO_2$ was saturated with triclosan, the valve was opened to spray the solution into the expansion chamber through a laser-drilled orifice nozzle with a hole. The nozzle used in this study was made of stainless steel 316 (150 μm thick and 9 mm outer diameter) and has inner diameters of 30 μm. The nozzle was heated using a heating tape. When the supercritical solutions were depressurized through the nozzle to ambient conditions, they rapidly expanded and the solute was re-crystallized. Solutes were collected in the chamber. An expanded CO_2 was vented off through a filter paper which was located at the bottom of the chamber.

2.4. PARTICLE ANALYSIS

Particle size and particle size distribution were analyzed directly in the laser diffraction beam as an aerosolized dry powder using RODOS dry powder accessory (Sympatec Gmbh, HELOS/BF). The measuring range of particle size was from 0.1 to 35 μm.

Particle morphology was analyzed by SEM (JEOL, JSM-6700F). The particles were initially spread on a carbon tape glued to an aluminum stub and coated with a silver to make the particle surface conductive to electrons by SEM. Particles were observed by SEM and the micrographs were taken and recorded.

3. CORRELATION

In this work, the experimental data for the CO_2 + triclosan system were correlated using the quasi-chemical nonrandom lattice fluid (QLF) EOS[10-12]. The QLF model and the fugacity coefficient of a component in mixture are expressed as follows:

$$\frac{\tilde{P}}{\tilde{T}} = -\ln(1-\tilde{\rho}) + \frac{z}{2}\ln[1+(\frac{q}{r}-1)\tilde{\rho}] - \frac{\theta^2}{\tilde{T}} \tag{1}$$

$$\ln\varphi_i = (Z-1)\frac{r_i}{r}(\frac{v_i^*}{v^*}-1) + r_i\frac{\tilde{P}}{\tilde{T}} - \frac{zq_i}{2}\ln(1+(\frac{q}{r}-1)\tilde{\rho}) - \ln Z + \frac{q_i\theta}{\tilde{T}}\left[\theta - \frac{2\sum_{j=0}^{c}\theta_j\varepsilon_{ij} + \beta\sum_{j=0}^{c}\sum_{k=0}^{c}\sum_{l=0}^{c}\theta_j\theta_k\theta_l\varepsilon_{ij}(\varepsilon_{ij}+2\varepsilon_{kl}-2\varepsilon_{jk}-\varepsilon_{ik})}{\theta\varepsilon_M}\right] \tag{2}$$

Here, all the quantities with the tilde (~) denote the reduced variables defined by

$$\tilde{P} = \frac{P}{P^*}, \quad \frac{T}{T^*}, \quad \tilde{\rho} = \frac{\rho}{\rho^*}, \quad \rho^* = \frac{1}{rv^*} \tag{3}$$

where the reducing parameters are defined by

$$P^*v^* = kT^* = \frac{z}{2}\varepsilon_M \tag{4}$$

and ε_M, θ are defined by

$$\varepsilon_M = \frac{1}{\theta^2}\left[\sum_{i=0}^{c}\sum_{j=0}^{c}\theta_i\theta_j\varepsilon_{ij} + \frac{\beta}{2}\sum_{i=0}^{c}\sum_{j=0}^{c}\sum_{k=0}^{c}\sum_{l=0}^{c}\theta_i\theta_j\theta_k\theta_l\varepsilon_{ij}(\varepsilon_{ij}+3\varepsilon_{kl}-2\varepsilon_{ik}-2\varepsilon_{jk})\right] \tag{5}$$

$$\theta = \frac{\sum N_i q_i}{N_q} = \frac{(q/r)\tilde{\rho}}{1+(q/r-1)\tilde{\rho}} = 1-\theta_0 \tag{6}$$

where ε_{ij} are defined by

$$\varepsilon_{ij} = \sqrt{\varepsilon_{ii}\varepsilon_{jj}}\ (1-k_{ij}) \tag{7}$$

The modeling of the solubility y_2 of a solid component (2) in a supercritical phase requires solving the following equilibrium relation:

$$y_2 = \frac{\varphi_2(T, P_2^{sub})P_2^{sub}(T)}{P\varphi_2(T,P,y_2)}\exp\left(\frac{v_2^S(P-P_2^{sub}(T))}{RT}\right) \tag{8}$$

where $P_2^{sub}(T)$ is the sublimation pressure of component (2) and v_2^S its molar volume at temperature T; it is assumed that v_2^S is independent on pressure P. The fugacity coefficients $\varphi_2(T,P_2^{sub})$ and $\varphi_2(T,P,y_2)$ are respectively those of components (2) as a pure species at $P_2^{sub}(T)$ and in the supercritical mixture at pressure P; they should be estimated using an equation of state.

4. RESULTS AND DISCUSSION

4.1. SOLUBILITY OF TRICLOSAN IN SUPERCRITICAL CO_2

The solubility of triclosan was measured by observing a cloud point at temperatures of 313.15, 323.15 and 333.15 K. The solubility data of triclosan in $scCO_2$ are given in Table 1. The properties of the pure CO_2 and triclosan are listed in Table 2. The

Table 1. Experimental data of triclosan solubility in scCO₂ at 313.15, 323.15 and 333.15 K

T (K)	P (MPa)	y_2
313.15	9.78	0.00009
	12.08	0.00014
	14.18	0.00022
	16.03	0.00027
	17.78	0.00040
	20.47	0.00055
	24.35	0.00093
	28.35	0.00142
	33.25	0.00231
323.15	12.05	0.00009
	13.53	0.00014
	15.27	0.00022
	16.33	0.00027
	18.65	0.00040
	20.54	0.00055
	23.69	0.00093
	27.55	0.00142
	31.54	0.00231
333.15	13.77	0.00009
	14.91	0.00014
	16.22	0.00022
	17.03	0.00027
	18.62	0.00040
	20.28	0.00055
	23.45	0.00093
	26.85	0.00142
	30.73	0.00231

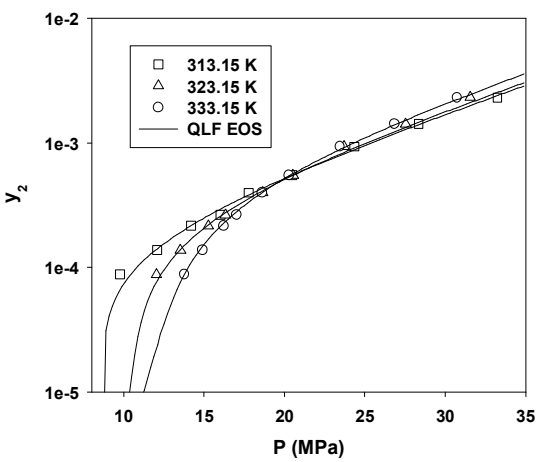

Figure 3. Solubility of triclosan in scCO₂ with the QLF EOS.
(□, 313.15 K ; △, 323.15 K; ○, 333.15 K)

Table 2. Pure properties of CO₂ and triclosan

Components	T_c (K)	P_c (MPa)	w
CO_2	304.21	7.38	0.224
Triclosan	884.52	3.33	0.744
Components	v^s (cm^3/mol)	A^{suba}	B^{suba}
CO_2	-	-	-
Triclosan	457.6	8.856	5203.2

Table 3. Molecular parameters for pure CO₂ and triclosan in QLF EOS

Components	v_i^* (cm^3/mol)	r_i	ε_{ii}/k (K)
CO_2	4.016	7.520	68.40
Triclosan	13.327	15.499	157.93

Table 4. Binary interaction parameters, k_{ij} and AADY of the QLF EOS for the CO₂ + triclosan system

Systems	T(K)	QLF EOS	
		k_{ij}	$AADy^*$
CO_2 + Triclosan	313.15	0.1156	0.0589
	323.15	0.1209	0.0546
	333.15	0.1215	0.0347

critical properties of triclosan were estimated from group contribution method, developed by Joback and Reid[15] and modified by Stein and Brown[16]. The sublimation pressures and molar volume of triclosan are calculated by group contribution method[17, 18]. There are 3 molecular parameters for pure fluids; unit cell volume (v_i^*), segment number (r_i), energy parameter (ε_{ii}) and single binary interaction parameter k_{ij} for mixture in QLF EOS. Pure parameters of CO2 are fitted to saturated liquid density, vapor pressure and P-V-T data from the Korea Thermophysical Properties Databank (KDB)[19]. Pure parameters of triclosan are fitted to vapor pressure from group contribution method[15]. Molecular parameters for pure CO2 and triclosan in QLF EOS are described in Table 4.

Binary interaction parameters k_{ij} were obtained by minimizing the Absolute Average Deviation of y_2 (AADy):

$$AADy = \frac{1}{N_{\exp}} \sum_{i}^{N_{\exp}} \left| \frac{y_{2i}^{\exp} - y_{2i}}{y_{2i}^{\exp}} \right| \tag{9}$$

where $y_{2i}^{\exp}$ and y_{2i} are the experimental solubilities of the solid in SCF and those calculated by means of EOS, respectively.

Table 5. RESS experiment conditions and results

Run no.	$T_{extraction}$ (K)	$P_{extraction}$ (MPa)	Average particle size x50(μm)
Raw	-	-	96.4
1	313.15	15.0	2.04
2	323.15	15.0	2.12
3	333.15	15.0	3.04
4	343.15	15.0	4.12
5	313.15	10.0	2.64
6	313.15	12.5	2.00
7	313.15	20.0	1.94

The experimental data were correlated well with the QLF EOS within 5.89 % ADDy for the CO_2 + triclosan system. The binary interaction parameters for this system are summarized in Table 3 together with AADy. The binary interaction parameters tend to slightly increase as temperature increases. Solubility increased as pressure increased at a constant temperature. These results can be explained as follows. As pressure is increased, carbon dioxide density increases and the intermolecular distance of carbon dioxide molecules decreased. The specific interaction between the solute and solvent molecules, therefore, is increased and solubility is improved. Also, a retrograde phenomenon is found. Below a crossover pressure, the solubility decreases as temperature increases, but, above the crossover pressure, the solubility increases as temperature increases. This phenomenon can be explained as follows. Temperature has an influence on a solute vapor pressure and solvent density. Below the crossover pressure, CO_2 density rapidly decreases as temperature increases at a constant pressure, and as CO_2 density is dominant, the solubility decreases. Above the crossover pressure, the CO_2 density barely influenced, because the pressure remains high. On the other hand, the solute vapor pressure increases as temperature increases and therefore, the solubility increases.

4.2. RECRYSTALLIZATION OF TRICLOSAN

The experiments were carried out to investigate the effect of extraction pressure and temperature on the size and morphology of triclosan particles obtained by the RESS process. The experimental conditions and results are reported in Table 5. The extraction pressure and temperature were determined according to the solubility data obtained for triclosan in $scCO_2$.

Figure 4 is an SEM image of the raw triclosan. The raw particle has a rectangular parallelepiped shape with a rounded edge and a smooth surface. Typical particle size of the raw particle was 100 μm in length and 20μm in width. The RESS processed particles are irregular and polyhedral in shape (Figure 5-6). The average particles sizes of processed particles are between 1.94 and 4.12 μm.

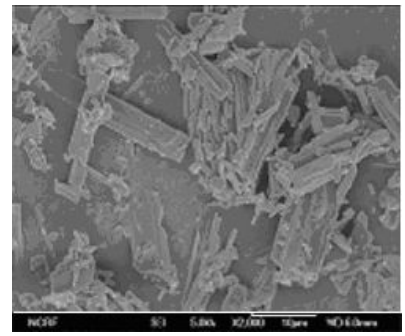

Figure 4. SEM image of the raw particles.

4.2.1. EFFECT OF TEMPERATURE

The effect of extraction temperature was studied for the range of 313.15 to 343.15 K at 15 MPa. SEM images are shown in Figure 5. As the extraction temperature increases the average particle sizes increase from 2.04 to 4.12 μm.

An increase of temperature decreases the CO_2 density and leads to a decrease of a solvent power. As a result, a lower supersaturation and lower nucleation are achieved. Consequently, particle size increases with temperature increases. Further, an increase of temperature cause to increase the solute's vapor pressure leading to higher solution concentration. The high concentration of the solution brings about the increase of the particle size as a consequence of the particle growth and coagulation

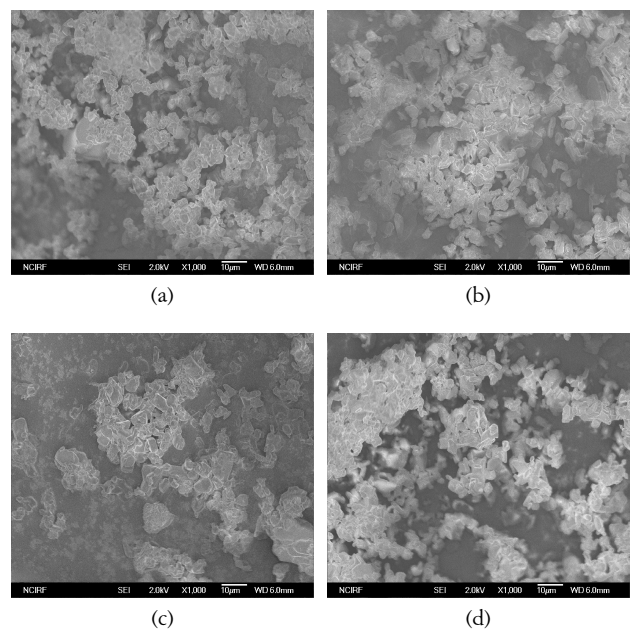

(a) (b) (c) (d)

Figure 5. SEM images of particles obtained by RESS at various temperatures at P = 15.0 MPa:
(a) $T_{extraction}$ = 313.15 K, (b) $T_{extraction}$ = 323.15 K; (c) $T_{extraction}$ = 333.15 K; (d) $T_{extraction}$ = 343.15 K.

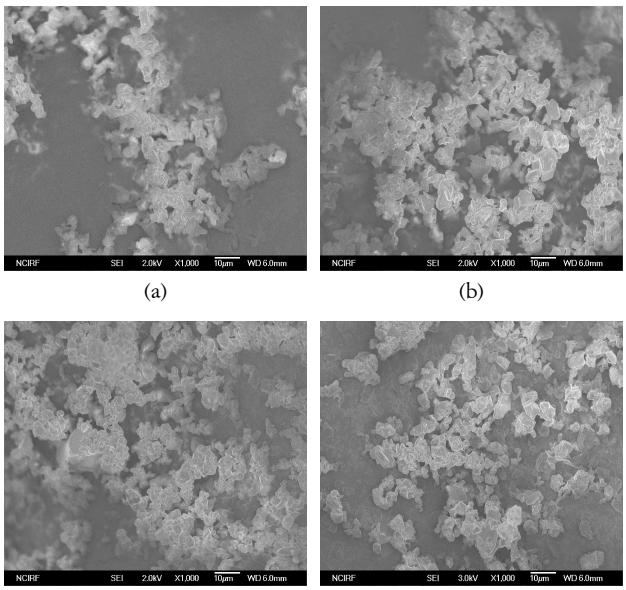

Figure 6. SEM images of particles obtained by RESS at various pressures at T = 313.15 K.
(a) $P_{extraction}$ = 10.0 MPa; (b) $P_{extraction}$ = 12.5 MPa; (c) $P_{extraction}$ = 15.0 MPa; (d) $P_{extraction}$ = 17.5 MPa.

among the particles.

4.2.2. EFFECT OF EXTRACTION PRESSURE

The effect of extraction pressure was studied for the range of 10 to 17.5 MPa. SEM images of the particles obtained different pressure given in Figure 6. Increasing in extraction pressure resulted in decrease in the average particle size (from 2.64 to 1.94 μm). The extraction pressure affects particle size in several aspects. First, the higher the pressure, the greater the solubility of triclosan in $scCO_2$ since the CO_2 density increases as pressure increases. The increase of the triclosan in $scCO_2$ solubility results in the greater the degree of supersaturation and higher nucleation rate. Second, higher pressure leads to a higher mass flow rate of the solution and causes reduced residence time in the nozzle. Consequently, time for particle growth will be decreased within a nozzle. Both phenomena can lead to a decreased particle size. Third, the higher the pressure, the higher the solution concentration, this frequently leads to coagulation among particles. As a result, the particle size increases. Therefore, it can be explained that the first and second phenomenon is dominant in this study.

5. CONCLUSION

The micronized triclosan particles were successfully prepared using the RESS process. In order to determine the condition of RESS experiment, the solubility of triclosan in $scCO_2$ was measured by a high pressure apparatus equipped with a variable volume view cell. We also extended the QLF EOS for the calculation of supercritical fluid phase equilibrium and correlated satisfactorily the solubility of triclosan in $scCO_2$ and investigated the effect of pressure and temperature on particles in RESS process. As the extraction pressure increased or the extraction temperature decreased, the average particle size decreased.

List of symbols

A	Helmholtz free energy
k	Boltzmann's constant
q	Surface area parameter
r	Number of segments per molecule
T	Temperature
V	Volume
v	Molar volume
v^*	Close packed volume of a mer
x	Liquid mole fraction
z	Lattice coordination number
Z	Compressibility factor

Greek letters

β	Reciprocal temperature $(1/kT)$
ε_{ij}	Molecular interaction energy for component i and j
ε_M	Molecular interaction energy defined by eq(5)
φ	Fugacity coefficient
ρ	Molar density
ρ^*	Close-packed molar density
θ	Surface area fraction

Superscript

~	Reduced properties
*	Characteristic properties

Acknowledgement

This work was supported by the BK21 project and by the National Laboratory (NRL) Program of Ministry of Education, Science and Technology of Korea.

References

1. Teja A. S., and Eckert C. A., "Commentary on Supercritical Fluids: Research and Applications," *Ind. Eng. Chem. Res*., **39**(12), 4442-4444 (2000).
2. Jung J., and Perrut M., "Particle Design Using Supercritical Fluids: Literature and Patent Survey," *J. Supercrit. Fluids*, **20**(3), 179-219 (2001).
3. Knez Z., and Weinder E., "Particles Formation and Particle Design Using Supercritical Fluids," *Curr. Opin. Solid State Mater. Sci.*, **7**(4-5), 353-361 (2003).

4. Kayrak D., Akman U., and Hortaçsu Ö., "Micronization of Ibuprofen by RESS," *J. Supercrit. Fluids*, **26**(1), 17-31 (2003).
5. Beckman E. J., "Supercritical and Near-critical CO_2 in Green Chemical Synthesis and Processing," *J. Supercrit. Fluids*, **28**(2-3), 121-191 (2004).
6. Huang Z., Sun G.-B., Chiew Y. C., and Kawi S., "Formation of Ultrafine Aspirin Particles Through Rapid Expansion of Supercritical Solutions (RESS)," *Powder Technol*., **160**(2), 127-134 (2005).
7. Howard M., "Pharmaceutical Compositions and Methods for Managing Skin Conditions," U.S. Patent No. 7,018,660 (2006).
8. Heath R. J., Rubin J. R., Holland D. R., Zhang E., Show M. E., and Rock C. O., "Mechanism of Triclosan Inhibition of Bacterial Fatty Acid Synthesis," *J. Biol. Chem.*, **274**(16), 11110-11114 (1999).
9. Peng D. Y., and Robinson D. B., "A New Two-constant Equation of State," *Ind. Eng. Chem. Fundam.*, **15**(1), 59-64 (1976).
10. Shin M.S., and Kim H. "A Qausi-chemical Nonrandom Lattice Fluid Model; General Derivation and Application to Pure Fluids and Mixtures," *Fluid Phase Equilibr.*, **246**(1-2), 79-88 (2006).
11. Shin M.S., and Kim H., "A A Qausi-chemical Nonrandom Lattice Fluid Model for Phase Equilibria of Associating systems," *Fluid Phase Equilibr.*, **256**(1-2), 27-33 (2007).
12. Shin, M. S., and Kim, H., "Solubility of Iodopropynyl Butylcarbamate in Supercritical Carbon Dioxide," *Fluid Phase Equilibr.*, **270**(1-2), 45-49 (2008).
13. Bae W., Kwon S., Byun H. S., and Kim H., "Phase Behavior of the Poly(vinyl pyrrolidone) + *N*-vinyl-2-pyrrolidone + Carbon Dioxide System," *J. Supercrit. Fluids*, **30**(2), 127-137 (2004).
14. Shin J., Shin M. S., Bae W., Lee Y. W., and Kim H., "High-pressure Phase Behavior of Carbon DioxideHeptadecafluoro-1-decanol System," *J. Supercrit. Fluids*, **44**(3), 260-265 (2008).
15. Joback K. G., and Reid R. C., "Estimation of Pure-component Properties from Group-Contributions," *Chem. Eng. Comm.*, **57**(1-6), 233-243 (1987).
16. Stein S. E., and Brown R. L., "Estimation of Normal Boiling Points from Group Contributions," *J. Chem. Inf. Comput. Sci.*, **34**(3), 581-587 (1994).
17. Lyman W. J., Reehl W. F., and Rosenblatt D. H., Handbook of Chemical and Physical Property Estimation Methods: Environmental Behavior of Organic Compounds, American Chemical Society, Washington, D.C. (1990).
18. Fedors R. F., "A Method for Estimation Both the Solubility Parameters and Molar Volume of Liquids," *Polym. Eng. Sci.*, **14**(2), 147-154 (1974).
19. Kang J., Yoo K. P., Kim H., Lee J., Yang D., and Lee C. S., "Development and Current Status of the Korea Thermophysical Properties Databank (KDB)," *Int. J. Thermophys.*, **22**(2), 487-494 (2001).